Chapter 9

Tempospatial Distribution, Gas: Solid Partition, and Long-Range Transportation of Atmospheric Mercury at an Industrial City and Offshore Islands

Yi-Hsiu Jen and Chung-Shin Yuan

Additional information is available at the end of the chapter

http://dx.doi.org/10.5772/intechopen.74051

Abstract

This chapter measured atmospheric mercury from two cases of small-scale regions to large-scale regions, and further investigated the tempospatial variation of atmospheric mercury, gas-particulate partition, the transportation routes of mercury, and the comparison of mercury concentration in urban areas and stationary sources. In a heavily polluted industrial city, Kaohsiung, field measurement results showed that total gaseous mercury (TGM) and Hg_p concentrations were in the range of 2.38–9.41 and 0.02–0.59 ng/m^3 with the highest concentrations of 9.41 and 0.59 ng/m^3, respectively. Moreover, the partition of atmospheric mercury was apportioned as 92.71–99.17% TGM and 0.83–7.29% Hg_p. The hot spots of atmospheric mercury were allocated at two regions in Kaohsiung City, including a steel industrial complex in the south and a petrochemical industrial complex in the north. In a coastal site of the Penghu Islands, the field measurement results showed that the average TGM concentration during the monitoring periods was 3.17 ± 1.17 ng/m^3 with the range of 1.17–8.63 ng/m^3, as the highest concentration being observed in spring, while the average TGM concentrations in the daytime were typically higher than that at nighttime. Therefore, prevailing wind direction and air mass transportation routes potentially played critical roles on the variation of TGM concentration at the Penghu Islands.

Keywords: atmospheric mercury, tempospatial variation, gas-particulate partition, backward trajectory simulation, long-range transportation

1. Introduction

The United States had already listed 189 hazardous air pollutants (HAPs) for control in Title III of the Clean Air Act Amendments (CAAA) of 1990 [1, 2]. Among them, 11 are the toxic

heavy metals As, Be, Cd, Co, Cr, Hg, Ni, Mn, Pb, Sb, and Se. In 2005, the U.S.A. Environmental Protection Agency (USEPA) became the first agency to amend the Maximum Achievable Control Technology (MACT) standards into growth control quotas for mercury emissions in order to increase the original goal of a 30% reduction in mercury emissions to 70% by 2018 [2]. This was also done to encourage countries around the world to revise their own reduction goals for mercury emissions. Till now, the pollutants of mercury still cannot be completely removed by using chemical method, and continue to endanger the health of humans and other organisms.

Mercury (Hg) is a persistent, toxic, and bio-accumulative heavy metal, and is currently regulated by the USEPA and the United Nations Environment Programme (UNEP) [3–10], and atmospheric mercury has been claimed by UNEP as another global environmental issue followed greenhouse gases (GHGs) [1, 2]. Because of its unique physicochemical properties and potential for long-range transportation via the atmospheric dispersion pathway, it could be deposited worldwide [4, 5]. Due to its characteristics of persistence and bioaccumulation through food chain, mercury could damage the brain and nervous systems in human body. Thus, many countries are becoming increasingly concerned about atmospheric mercury pollution recently.

Accordingly, this chapter aimed to investigate the tempospatial variation and partition of atmospheric mercury at an industrial metropolitan area, and to explore the long-range transportation path at the marine boundary layer (MBL), and to compare the atmospheric mercury concentration level with other major cities all over the world.

2. Tempospatial variation and partition of atmospheric mercury in ambient air of an industrial city

2.1. Background

The mercury emission was mainly generated from combustion sources and metallurgy smelting processes in Taiwan. Among them, the combustion sources include coal-fired boilers, municipal and industrial waste incinerators, petrochemical refineries, cremators, etc., while the metallurgy smelting processes include integrated steel plants, electric arc furnace plants, secondary metal smelters, etc. The economic development of metro Kaohsiung mainly relied on heavy industries located adjacent to the metropolitan area. Coupled with heavy traffics, it causes poor ambient air quality of Kao-Ping Air Quality Zone in Taiwan. Moreover, metro Kaohsiung is the largest and most intensive industrial city in Taiwan, accounting for about 70% of the stationary emission sources, where has two large-scale coal-fired power plants, an integrated steel plant, several metallurgy smelters, and three petrochemical refineries. It would cause quite high emissions of mercury in metro Kaohsiung, Taiwan. In this chapter, the field measurement of atmospheric mercury was designated to investigate the tempospatial variation and partition of gaseous and particulate mercury during the wet and dry seasons, and further correlated atmospheric mercury with meteorological parameters and criteria air pollutants measured in Kaohsiung City, located at the coastal region of southern Taiwan.

2.2. Selection and description of sampling sites

Field measurement of atmospheric mercury speciation and concentration was conducted at a coastal background site and six sensitivity sites in Kaohsiung City, including Nan-zhi (22°44′00″ North latitude, 120°19′41″ East longitude, S1), Ren-wu (22°41′20″ North latitude, 120°19′57″ East longitude, S2), Zuoying (22°40′29″ North latitude, 120°17′34″ East longitude, S3), Cia-jin (23°37′56″ North latitude, 120°17′16″ East longitude, S4), Cianjhen (22°36′18″ North latitude, 120°18′30″ East longitude, S5), and Hsiao-kang (22°33′57″ North latitude, 120°20′15″ East longitude, S6). The coastal background site along coastline far away from the emission sources is located at the campus of National Sun Yat-Sen University (22°37′38″ North latitude, 120°16′01″ East longitude). The location of the coastal background site and six sensitivity sites for sampling total gaseous mercury (TGM) and particulate mercury (Hg_p) in Kaohsiung City is shown in **Figure 1**.

These sensitivity sites were mainly located at the ambient air quality monitoring stations in Kaohsiung City. Among them, sites S5–S6 were nearby a steel industrial complex in southern Kaohsiung, sites S1 and S2 were close to a petrochemical industrial complex in northern Kaohsiung. Active sampling of TGM and Hg_p were conducted consecutively for 24 h at each site in the wet and dry seasons from June to December of 2010 in Kaohsiung City. Among them, wet season started from June to September, while dry season started from October to December. This study intended to investigate the seasonal variation, the spatial distribution, and the partition of TGM and Hg_p at a coastal background site and six sensitivity sites in an industrial city.

2.3. Seasonal variation and partition of TGM and Hg_p

Figure 2 illustrates the seasonal variation of TGM and Hg_p concentrations at the northern and southern Kaohsiung as well as the coastal background site during the wet and dry

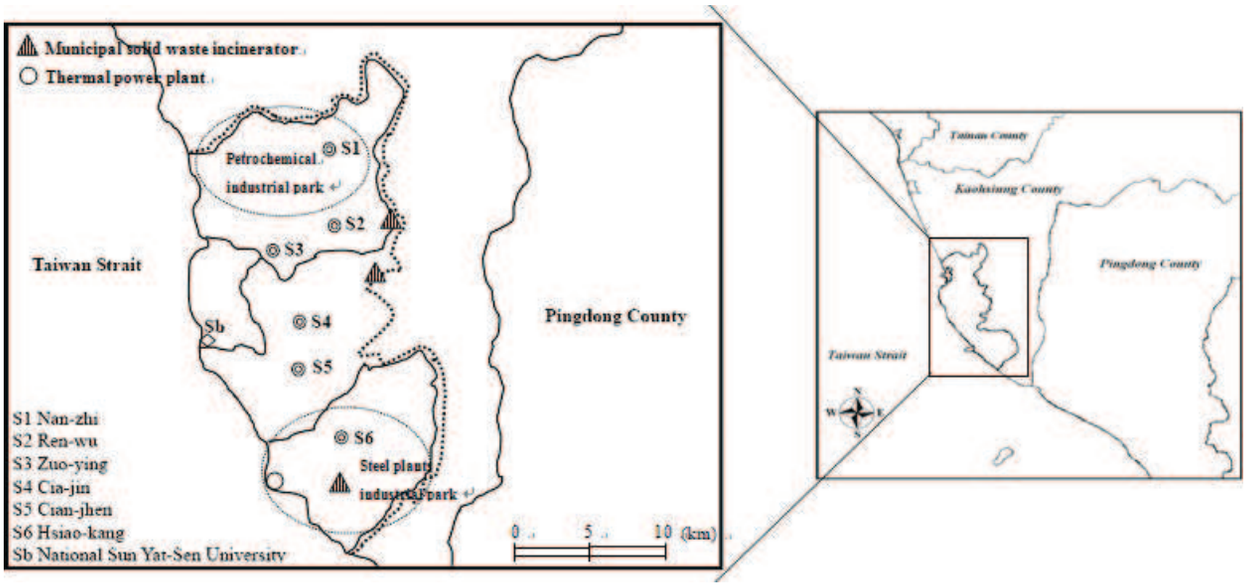

Figure 1. The location of six sensitivity sites and the coastal background site for TGM and Hg_p sampling in Kaohsiung City.

seasons. The field measured meteorological data are listed in **Table 1**, and the field measurement data with mean, standard deviation (SD), and partition of TGM and Hg_p are summarized in **Table 2**.

During the wet season, ambient temperature, relative humidity, wind speed, and UV_B were 28.9 ± 0.7°C, 78.3 ± 1.7%, 2.2 ± 0.2 m/s, and 3.4 ± 0.5 UVI, respectively, which were mostly higher than those during the dry season (**Table 2**). The prevailing wind blew from southwest and northeast during the dry season, and the prevailing wind blew from northwest and northeast during the wet season were reported. It was mainly attributed to the fact that

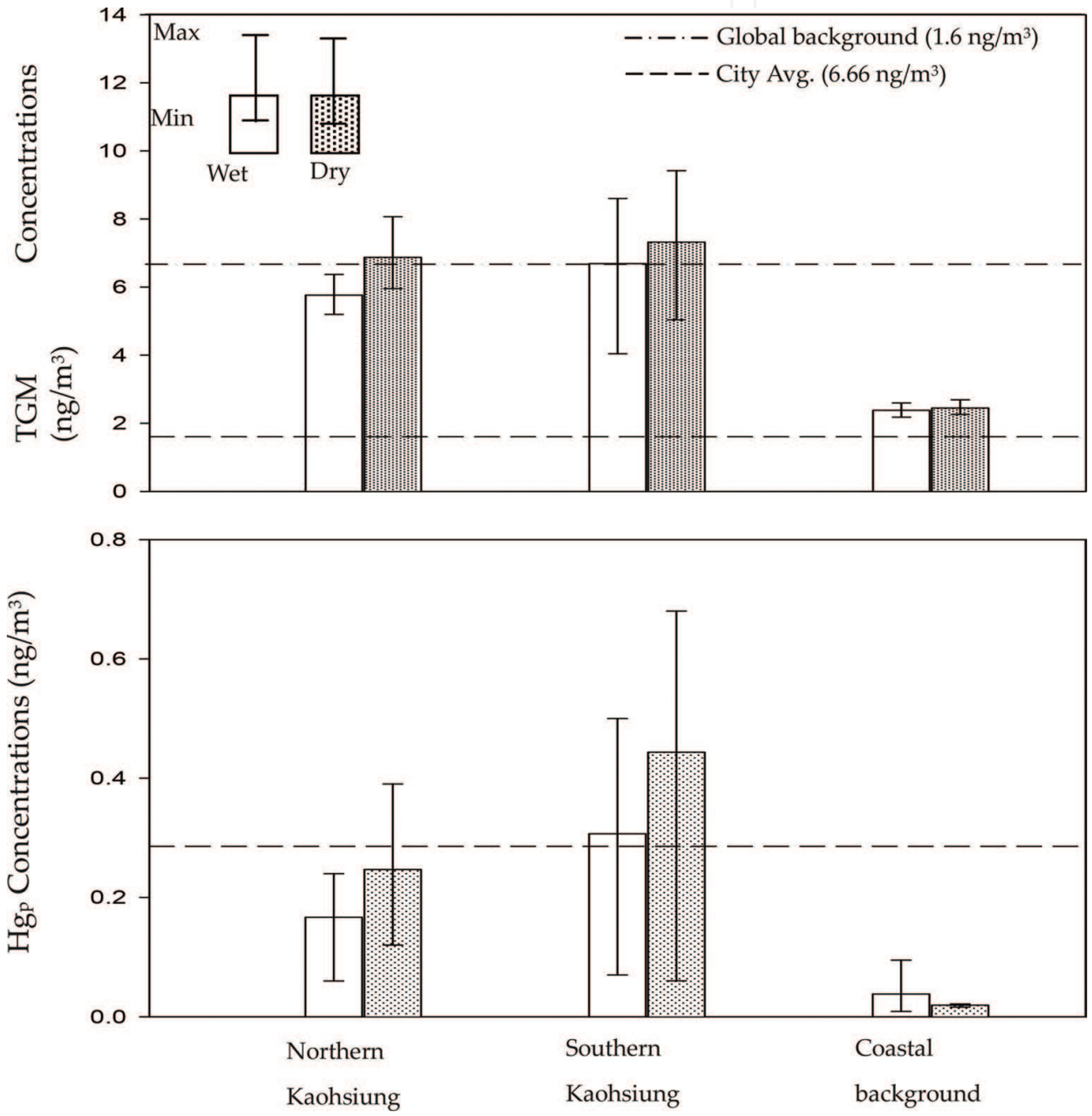

Figure 2. Tempospatial variation of TGM and Hg_p concentrations during the wet and dry seasons in the northern and southern Kaohsiung sites and the coastal site.

Seasons	Temp. (°C)	RH (%)	Rainfall (mm)	Rainy days	UV_B (UVI)	WS (m/s)	WD
Wet	28.9 ± 0.7	78.3 ± 1.7	427.9 ± 305.1	50	3.4 ± 0.5	2.2 ± 0.2	SW, NE
Dry	23.7 ± 3.4	73.3 ± 3.1	63.0 ± 97.6	12	2.1 ± 0.3	1.9 ± 0.1	NW, NE

Temp.: ambient temperature; RH: relative humidity; Rainy days: days with rainfall ≧ 0.01 mm; WS: wind speed; WD: wind direction; UV_B: ultra-violet radiation.

Table 1. Meteorological parameters monitored in Kaohsiung City during the atmospheric mercury sampling periods for wet and dry seasons.

sea-land breezes blew frequently in Kaohsiung City. However, the wet season is the heat convection season (i.e., hurricane season), in which the rainfall was about 427.9 ± 305.1 mm and the rainy days (rainfall ≧ 0.01 mm) were about 50 days. The dry season commonly blew the northeast monsoon, in which the rainfall and rainy days were much less than those during the wet season. Therefore, the aforementioned meteorological condition is considered as the differential between the dry and wet seasons in Kaohsiung City.

Field measurement data showed that the concentrations of TGM and Hg_p were 6.23 ± 1.62 ng/m^3 and 0.23 ± 0.17 ng/m^3, respectively, during the wet season, while the concentrations of TGM and Hg_p were 7.09 ± 1.57 ng/m^3 and 0.35 ± 0.25 ng/m^3, respectively, during the dry season in Kaohsiung City. The concentrations of atmospheric mercury during the dry season was obviously higher than those during the wet season. It showed that meteorological condition and atmospheric dispersion played a critical role on the seasonal variation of atmospheric mercury concentration. However, the seasonal concentrations of TGM and Hg_p did not vary

Seasons	Types of Hg	Northern Kaohsiung sites			Southern Kaohsiung sites			Coastal background site
		S1	S2	S3	S4	S5	S6	Sb
Wet season (n = 12)	TGM (ng/m^3)	5.72	6.37	5.20	4.04	7.42	8.60	2.38
	Hg_p (ng/m^3)	0.20	0.24	0.06	0.05	0.35	0.50	0.02
	Mean ± SD (ng/m^3)	TGM		6.23 ± 1.62				
		Hg_p		0.23 ± 0.17				
Dry season (n = 12)	TGM (ng/m^3)	5.95	8.06	6.59	5.03	7.50	9.41	2.44
	Hg_p (ng/m^3)	0.23	0.39	0.12	0.08	0.59	0.68	0.03
	Mean ± SD (ng/m^3)	TGM		7.09 ± 1.57				
		Hg_p		0.35 ± 0.25				
Mean ± SD of atmospheric mercury (ng/m^3)		TGM		6.66 ± 1.42				2.41 ± 0.04
		Hg_p		0.29 ± 0.21				0.03 ± 0.01

S1: Nan-zhi site; S2: Ren-wu site; S3: Zuo-ying site; S4: Cia-jin site; S5: Cian-jhen site; S6: Hsiao-kang site; Sb: coastal site.

Table 2. Seasonal variation of TGM and Hg_p concentrations at six sensitivity sites and the coastal background site in Kaohsiung City.

much at the coastal background site, thus the seasonal variation has insignificant influences on regions where atmospheric mercury concentrations were high.

The atmospheric mercury concentrations at southern Kaohsiung were mostly higher than those at northern Kaohsiung during the wet and dry seasons, and their average concentrations were respectively 1.12 and 1.79 times of those at northern Kaohsiung. As a whole, the average concentrations of TGM and Hg_p in Kaohsiung City were about 2.94 and 11.7 times, respectively, higher than those at the coastal background site during the wet season, and were about 2.6 and 11.5 times, respectively, during the dry season. Overall, the average TGM and Hg_p concentrations were 6.66 ± 1.42 and 0.29 ± 0.21 ng/m^3, respectively, in Kaohsiung City. The TGM concentration in Kaohsiung City was about 4.2 times and 2.8 times higher than the background TGM concentration of the North Hemisphere (1.6 ng/m^3) and at the coastal background site in Kaohsiung City (2.4 ng/m^3), respectively. It showed that Kaohsiung City as a heavy industrial city was highly polluted by atmospheric mercury.

Figure 3 illustrates the partition of Hg_p during the wet and dry seasons in Kaohsiung City. The results showed that TGM was the main mercury species, accounting for 94.56–99.59% of atmospheric mercury during the wet season, and 92.71–99.37% of atmospheric mercury during the dry season. Furthermore, Hg_p concentration had a tendency to increase with the distance from the emission sources. The maximum partition of Hg_p were up to 20–40% of total atmospheric mercury (TAM) in the ambient air [11–13]. The partition of Hg_p was generally lower than 1% of TAM in the rural areas, about 1–3% in the metropolitan areas, and beyond 5% in the industrial areas [14–16]. **Figure 1** shows that site Sb is in the rural area, sites S3 and S4 are in the metropolitan areas, and other four sites are in the industrial areas in Kaohsiung City. Moreover, the partition of Hg_p during the dry season was higher than that during the wet season. It implied that the amount of rainfall, the number of rainy days, and relative humidity might correlate to the partition of Hg_p.

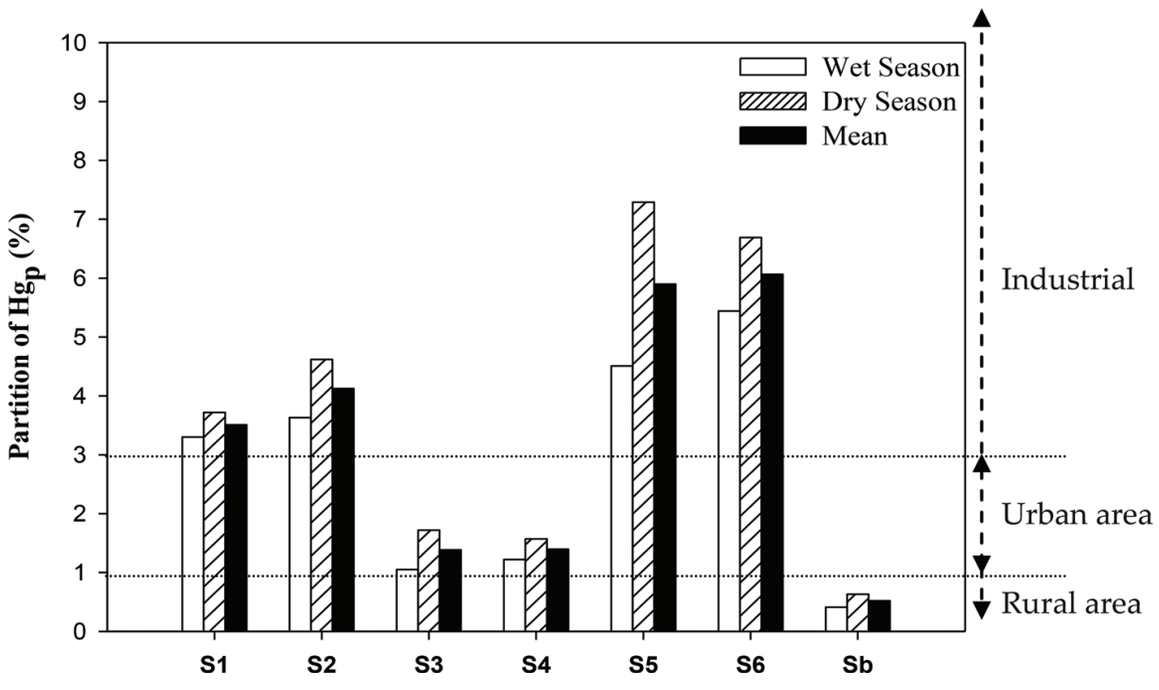

Figure 3. Partition of Hg_p during the wet and dry seasons at six sensitivity sites (S1–S6) and the coastal site (Sb).

2.4. Spatial distribution of TGM and Hg_p

The concentrations of TGM and Hg_p measured at each site are summarized in **Table 2**. As far as the spatial distribution of atmospheric mercury during the wet and dry seasons in Kaohsiung City was concerned, the atmospheric mercury concentrations (TGM of 6.37 ng/m^3; Hg_p of 0.24 ng/m^3) at site S2 was the highest and followed by sites S1 and S3 in northern Kaohsiung, while those (TGM of 8.60 ng/m^3; Hg_p of 0.50 ng/m^3) at site S6 was the highest and followed by sites S5 and S4 in southern Kaohsiung. During the dry season, the atmospheric mercury concentrations (TGM of 8.06 ng/m^3; Hg_p of 0.39 ng/m^3) at site S2 was also the highest and followed by sites S3 and S1 in northern Kaohsiung, while those (TGM of 9.41 ng/m^3; Hg_p of 0.50 ng/m^3) at site S6 was the highest and followed by sites S5 and S4 in the southern Kaohsiung.

The mapping software (SURFER) was further used for plotting the concentration contour of atmospheric mercury in Kaohsiung City. This software uses the grid difference as the calculation basis, and interpolarates the data of atmospheric mercury concentration obtained from each sampling site into the map of Kaohsiung City. This study aimed to explore the spatial distribution of atmospheric mercury concentration in Kaohsiung City. As shown in **Figure 4**, the atmospheric mercury concentrations of northern and southern Kaohsiung were obviously

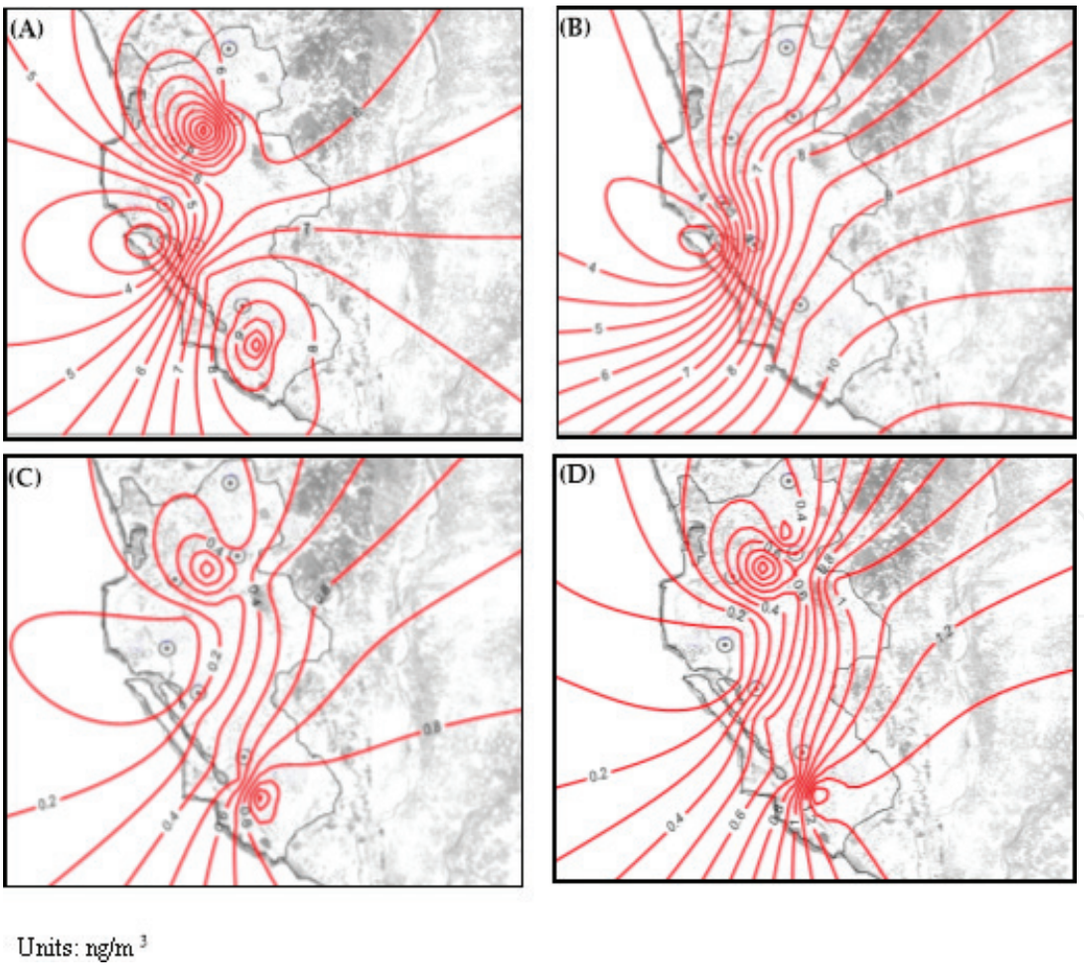

Figure 4. Spatial distribution of atmospheric mercury in Kaohsiung City. (A) TGM concentration during the dry season, (B) TGM concentration during the wet season, (C) Hg_p concentration during the dry season, and (D) Hg_p concentration during the wet season.

affected by the mercury emission sources. Two major high mercury concentration regions concurred with the petrochemical industrial district in northern Kaohsiung and the steel manufacturing complex in southern Kaohsiung. The main emission sources in northern Kaohsiung were petrochemical manufacturing complex, municipal and industrial waste incinerators, cremators, etc. In southern Kaohsiung, mercury was mainly emitted from steel smelters, electric arc furnaces, cement plants, petroleum refineries, coal-fired power plants, municipal waste incinerators, etc. Consequently, the atmospheric mercury concentration in southern Kaohsiung was higher than that in northern Kaohsiung, which was attributed to higher mercury emission in southern Kaohsiung than that in northern Kaohsiung. As a whole, the ambient air quality of Kaohsiung City was highly affected by the heavily densed industries, thus the concentration of atmospheric mercury in the metropolitan area was much higher than the background level during the wet and dry seasons. Both numbers of the emission sources and the consumption of fossil fuels in southern Kaohsiung were higher than those in northern Kaohsiung.

2.5. Comparison of TGM and Hg_p levels with other stationary sources

Figure 5 compares the concentrations of TGM and Hg_p at different mercury emission sources in southern Taiwan [12, 13]. The highest TGM concentrations were observed at a steel plant, which was approximately 2.6 times higher than those at Tainan Scientific Complex, even up to 15 times for Hg_p concentration. Similarly, other stationary sources were also higher than those observed at Tainan Scientific Complex for both TGM and Hg_p concentrations. **Figure 6** illustrates the partition of TGM and Hg_p for various mercury emission sources in southern Kaohsiung.

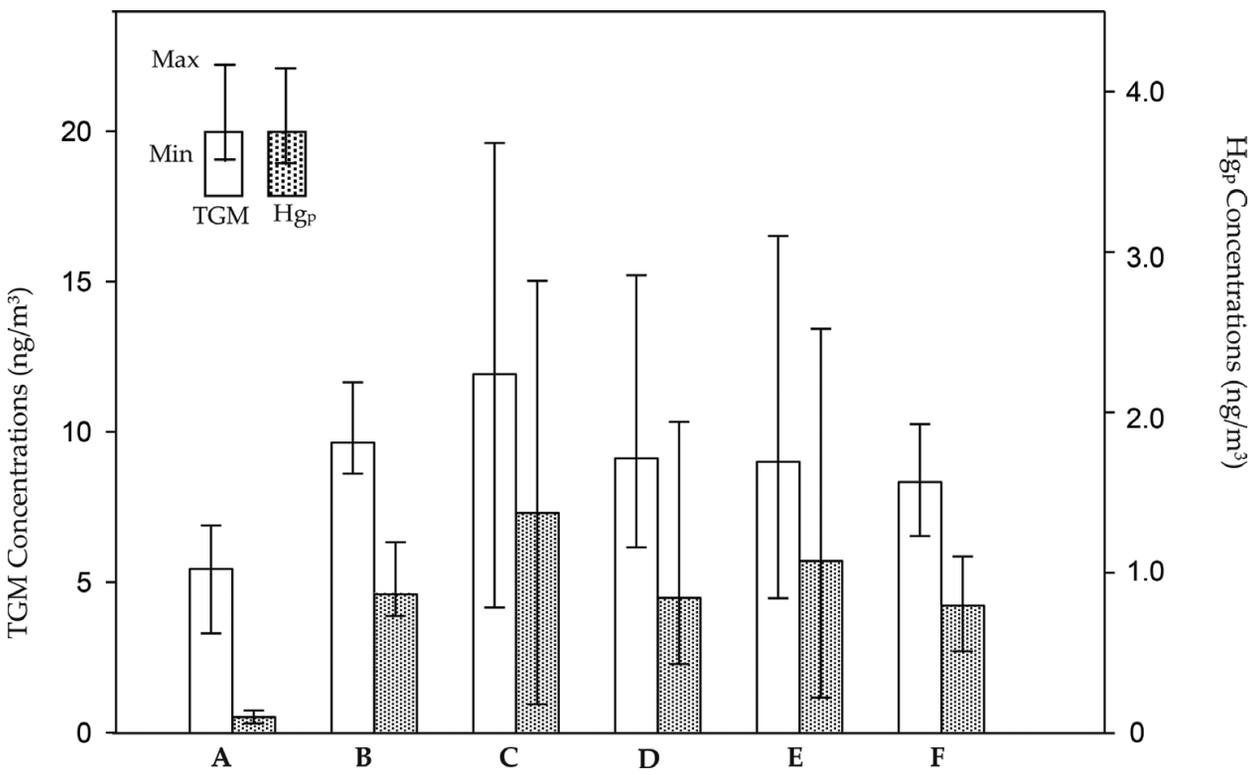

Figure 5. Comparison of TGM and Hg_p concentrations with various mercury emission sources in southern Kaohsiung (A: the semi-conductor complex, B: the petroleum refinery, C: the steel plant, D: the coal-fired power plant, E: the electric arc furnace, F: the municipal waste incinerator).

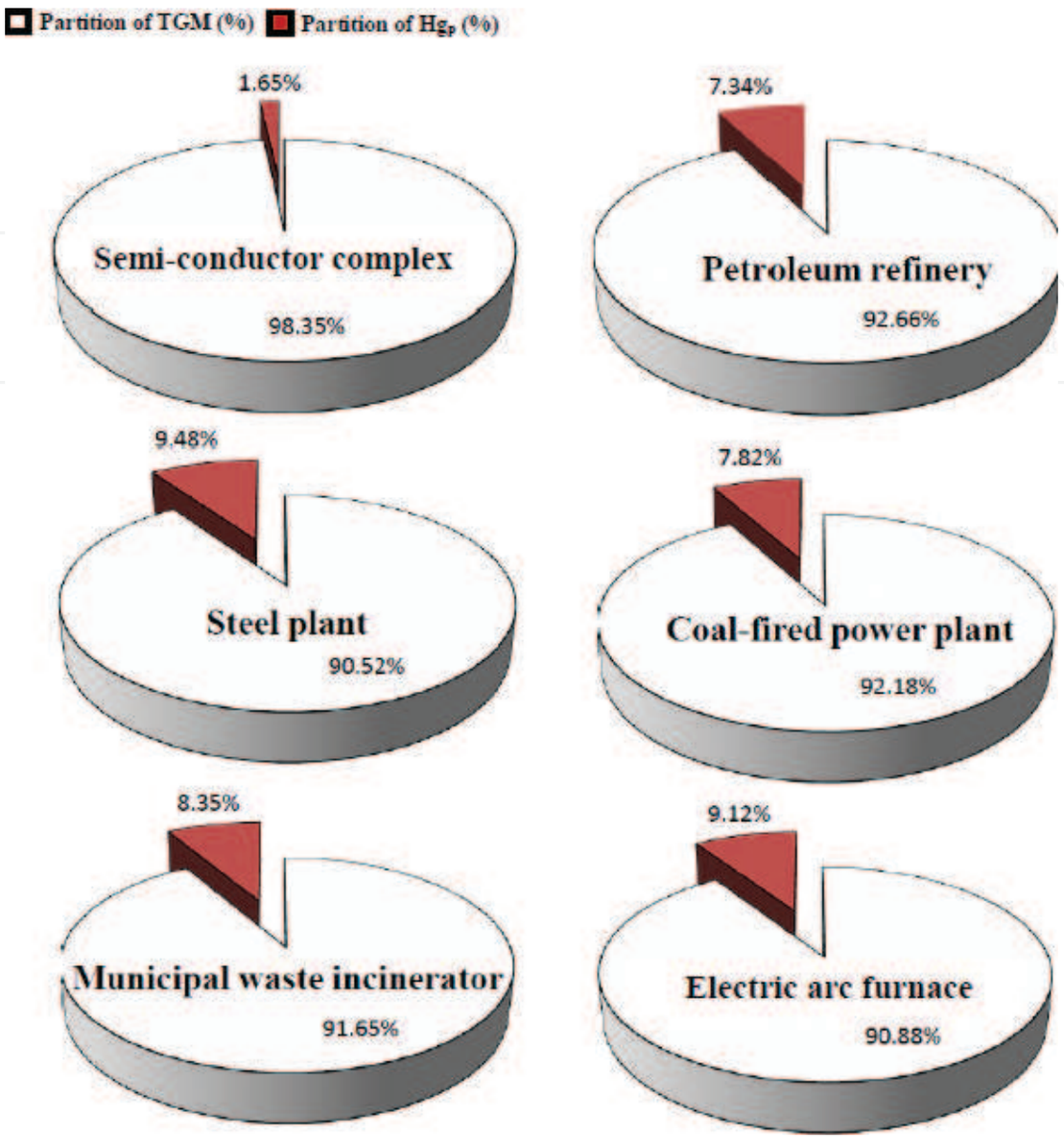

Figure 6. Location of the TGM monitoring site (★) at the Penghu Islands.

The partition of Hg_p at Tainan Scientific Complex was only 1.7%, which was similar to those observed at most urban areas (1–3%), and was much lower than other stationary sources (e.g., coal fired power plants, waste incinerators, and steel plants). Their partition of Hg_p ranged from 7.3 to 9.5%, which contributed much more Hg_p to the ambient air [6, 15, 17, 18]. Overall speaking, TGM was the dominant species of atmospheric mercury in southern Taiwan.

3. Total gaseous mercury concentration at marine boundary layer and associated long-range transportation

3.1. Background

Penghu Islands are located at the middle of the Taiwan Strait between the southeastern China and Taiwan. The islands are dominated by subtropical weather and mainly influenced by East

Asian monsoons. Previous studies reported that, during the seasons of spring and winter, the biomass and fossil fuel burning frequently occurring in Southeast Asia and Southwest China increase the levels of atmospheric mercury in Taiwan owning to long-range transportation [11, 18]. Since there are no significant mercury sources at the Penghu Islands, it can be treated as the background site in the region.

In this chapter, a one-year field monitoring protocol was conducted to investigate the seasonal and daily variations of TAM concentration at the Penghu Islands, as the correlation of TGM concentration with the meteorological parameters and several criteria air pollutants being further examined and discussed. More importantly, a backward trajectory simulation model was further applied to explore the transportation of TGM to the Penghu Islands with respect to the transportation routes for those observed at 500 m above the sea level during the monitoring seasons. While the TGM has been a continuing issue of great concern worldwide, the results of this study would help development more effective management strategies to control the adverse influences associated with the effect of TGM on the environment and human health as well in the Penghu Islands and the areas possibly affected by the long-range transportation of TGM.

3.2. Monitoring sites

According to the meteorological data obtained from 1985 to 2011, dry season with the rainfall of about 800 mm started from April to September. **Table 3** summarizes the meteorological data measured at the Penghu Islands during the TGM monitoring seasons, indicating that the prevailing winds were blown from the east, northeast, northwest, and south, with the ambient temperatures of 13.4–31.2°C, the relative humidity of 53.2–91.3%, and the wind speeds of 0.5–9.7 m/s. The TGM monitoring site was located on the roof of a four-floor building, which was approximately 12 m above the ground and 50 m and 500 m far from the coastline and the major roads, respectively. Overall, the TGM monitoring site was located at the marine boundary layer (MBL), reducing the possible interferences resulted by Hg emission sources. The atmospheric TGM was continuously monitored at the Hsiaomen site (23°38′471″ North latitude, 119°30′316″ East longitude) located at the northwestern coastline of the Penghu Islands (see **Figure 7**) for 15 continuous days in each season from March of 2011 to February of 2012.

Seasons	n	Temp. (°C)	RH (%)	WS (m/s)	WD
Spring	360	19.9 ± 2.1	72.5 ± 7.5	4.5 ± 2.2	ENE
Summer	360	29.8 ± 0.6	79.3 ± 2.7	2.2 ± 0.6	S
Fall	360	24.8 ± 0.6	75.1 ± 4.9	6.1 ± 1.5	ENE
Winter	360	16.1 ± 1.5	82.2 ± 4.7	6.2 ± 1.3	ENE
Mean ± SD		22.7 ± 5.9	77.3 ± 4.3	4.8 ± 1.9	—
Max		33.2	91.3	9.7	—
Min		13.4	53.2	0.5	—

Temp.: ambient temperature; RH: relative humidity; WS: wind speed; WD: wind direction; SD: standard deviation.

Table 3. Meteorological data recorded at the Penghu Islands during the TGM sampling periods.

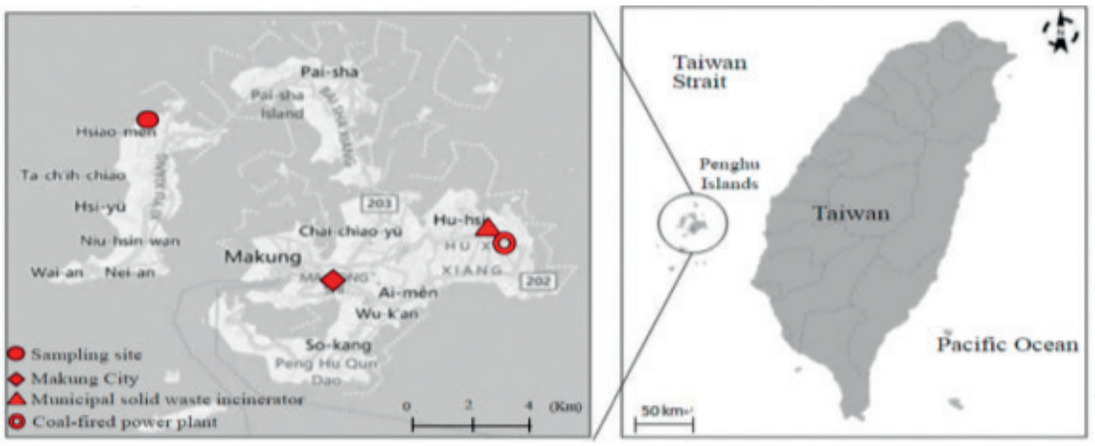

Figure 7. Variation of TGM concentration during four monitoring seasons at the Penghu Islands.

This chapter collected the meteorological data and the criteria air pollutant concentrations from the Makung Air Quality Station during the TGM monitoring periods, and discussed the correlation coefficients derived from the TGM concentrations with the meteorological parameters and the criteria air pollutants. Among them, the correlation coefficient (R) was used to describe the correlation between TGM concentration, meteorological data, and criteria air pollutant concentrations. The meteorological parameters included the ambient temperature (Temp.), relative humidity (RH), wind speed (WS), and wind direction (WD), while the criteria air pollutants of interest included SO_2, NO_X, CO, O_3, PM_{10}, and $PM_{2.5}$. Four seasons are defined as March to May (spring), June to August (summer), September to November (fall), and December to February (winter), respectively. 72-h backward trajectories were simulated by using a NOAA HYSPLIT model with the National Centers for Environmental Prediction's Global Data Assimilation System (NCEP-GDAS) meteorological dataset used as the model input in this study. All backward trajectories started with an arrival height of 500 m above the sea level. By using the NOAA-HYSPLIT model, the dates of the highest TGM concentration at the Penghu Islands in different seasons were determined and the transportation routes of air masses toward the Penghu Islands during the monitoring periods were then simulated.

This information was further applied to examine the possible transportation routes conveying TGM from the upwind sources to the Penghu Islands. Additionally, we used the local fire map to identify the possible sources of TGM drawn by the FIRMS web (http://firms.modaps.eosdis.nasa.gov/firemap/) with the moderate resolution imaging spectroradiometer (MODIS) data from National Aeronautics and Space Administration (NASA), which could illustrate the region and status of biomass burning during the monitoring periods.

3.3. Seasonal and daily variation of TGM concentration

Table 4 summarizes the average and standard deviation of TGM and criteria air pollutant concentrations measured at the Penghu Islands. The highest concentrations of PM_{10} and $PM_{2.5}$ observed in spring were 54.60 ± 15.56 and 31.07 ± 10.59 μg/m^3, respectively, while the lowest concentrations of PM_{10} and $PM_{2.5}$ occurred in summer were 36.63 ± 8.69 and 17.70 ± 6.48 μg/m^3, respectively. Spring and winter are two major seasons frequently blowing Asian dusts from

Seasons	n	TGM (ng/m³)	PM_{10} (μg/m³)	$PM_{2.5}$ (μg/m³)	SO_2 (ppb)	NOx (ppb)	O_3 (ppb)	CO (ppm)
Spring	360	4.31 ± 1.87	54.60 ± 15.56	31.07 ± 10.59	1.70 ± 0.72	5.61 ± 0.08	61.58 ± 5.00	0.27 ± 0.06
Summer	360	1.81 ± 0.15	36.63 ± 8.69	17.70 ± 6.48	2.21 ± 0.63	6.15 ± 1.23	33.17 ± 7.70	0.15 ± 0.03
Fall	360	3.03 ± 0.40	45.24 ± 18.49	21.40 ± 6.08	1.68 ± 0.52	3.48 ± 0.46	51.86 ± 5.99	0.18 ± 0.04
Winter	360	3.51 ± 0.67	48.65 ± 9.79	23.81 ± 12.18	2.00 ± 0.08	5.48 ± 1.63	38.59 ± 5.87	0.28 ± 0.08
P-value		3.32×10^{-55}	6.94×10^{-3}	1.93×10^{-3}	1.91×10^{-1}	1.36×10^{-7}	4.00×10^{-18}	3.04×10^{-10}
Mean ± SD		3.17 ± 1.06	46.28 ± 7.51	23.50 ± 5.64	1.90 ± 0.25	5.18 ± 1.17	46.30 ± 12.86	0.22 ± 0.06
Range		1.17–8.63	17.18–77.68	1.32–63.07	1.02–8.63	2.43–14.09	11.35–88.08	0.16–0.57

The concentrations observed among the seasons were significantly different by the analysis of ANOVA (Analysis of Variance) at the confidence level of 95%.

Table 4. Continuous monitoring data of TGM concentrations and their mean, standard deviation (SD), range, and the concentrations of criteria air pollutants.

http://dx.doi.org/10.5772/intechopen.74051

the northern China to the Penghu Islands [19], which significantly increased the concentrations of PM_{10}. Overall speaking, the concentrations of SO_2 and NO_x measured at the Penghu Islands were much lower than other cities in Taiwan, indicating no significant local sources in the Penghu Islands. Moreover, O_3 concentration was relatively higher compared to other criteria air pollutants at the Penghu Islands.

Field monitoring of TGM at the Penghu Islands showed that the average concentration of TGM was 3.17 ± 1.06 ng/m^3 with the range of 1.17–8.63 ng/m^3. The concentration of TGM in four monitoring seasons were ordered as: spring (4.34 ± 1.87 ng/m^3) > winter (3.51 ± 0.67 ng/m^3) > fall (3.03 ± 0.40 ng/m^3) > summer (1.81 ± 0.15 ng/m^3). Moreover, the average TGM concentration (3.17 ng/m^3) at the Penghu Islands was approximately two times of the background TGM concentration of North Hemisphere (1.6 ng/m^3). The Penghu Islands are likely to be influenced by long-range transportation of TGM in spring and winter, causing higher TGM concentrations in spring and winter than those in summer and fall. The lowest seasonal average TGM concentration of 1.81 ± 0.15 ng/m^3 was observed in summer, which was slightly close to the background TGM concentration of North Hemisphere, suggesting that air masses blown from the South China Sea were relatively clean.

Figure 8 illustrates the variation of TGM concentrations during the four monitoring seasons at the Penghu Islands. The daily concentration of TGM in spring increased significantly from April 2nd to the peak TGM concentration (8.63 ng/m^3) observed on April 10th. The lowest TGM concentration ranging from 1.50 to 2.70 ng/m^3 was compatibly observed in summer. Moreover, the concentrations of criteria air pollutants were also the lowest in summer compared to other seasons (**Table 4**), suggesting that the ambient air quality in summer was relatively better than other seasons at the Penghu Islands, and the TGM concentrations was 1.7–2.8 times lower than other seasons.

Unlike other seasons, the TGM concentrations fluctuated frequently in fall and winter. In winter, it increased rapidly from 3.74 to 5.08 ng/m^3 on December 28th, and then decreased

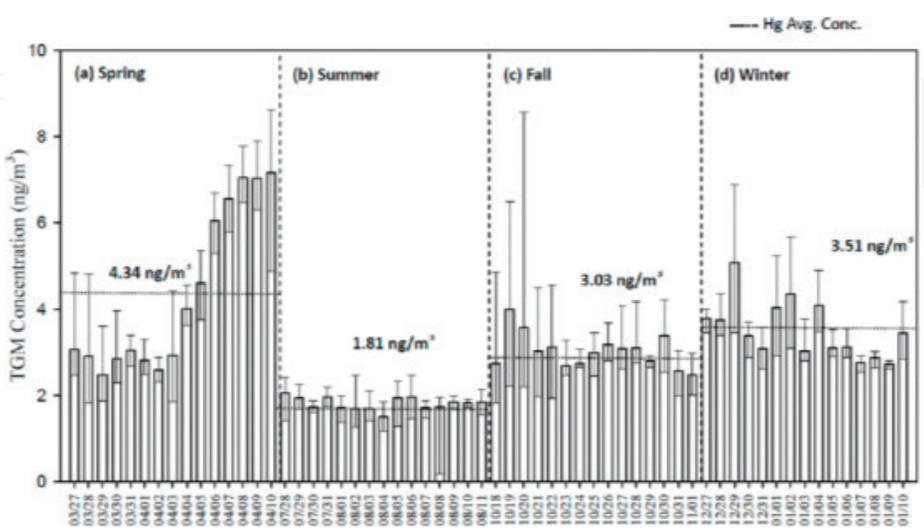

Figure 8. Hourly variation of TGM concentrations during four monitoring seasons at the Penghu Islands.

to 3.38 ng/m^3 on December 30th. The highest peak concentration (4.35 ng/m^3) occurred on December 29th and then leveled off on January 5th. Long-term TGM monitoring at Mt. Lulin background air quality monitoring station showed that Taiwan was highly influenced by atmospheric mercury and gaseous pollutants from China and Southeast Asia in spring and winter [11]. Backward trajectory simulation results indicated that the atmospheric mercury detected in Taiwan significantly increased due to frequent biomass burning originated from the Southeast Asia and industrial emissions from the North China in spring and winter. It suggested that the TGM concentrations at the Penghu Islands might be also influenced by the atmospheric mercury emitting and transporting from these regions. While, air masses blown from the Pacific Ocean had relatively low contribution to the TGM concentration.

3.4. Hourly variation of TGM concentration

Figure 9 illustrates the hourly variation of TGM concentrations during four seasons at the Penghu Islands. It showed that the variation of hourly TGM concentrations were relatively steady in summer. The TGM concentration increased from 6:00 am, gradually reached its concentration peak at 11:00 am, and then decreased after noontime. The increase of TGM concentration resulted probably from the following two processes: (a) UV radiation could temporally transform Hg^+, Hg^{2+}, and Hg_p to volatile Hg^0, and subsequently entered to the atmosphere [6]); (b) the downward mixing from the enhanced TGM aloft may increase the levels of TGM concentration as the destroying of nocturnal inversion layer [20]. Except

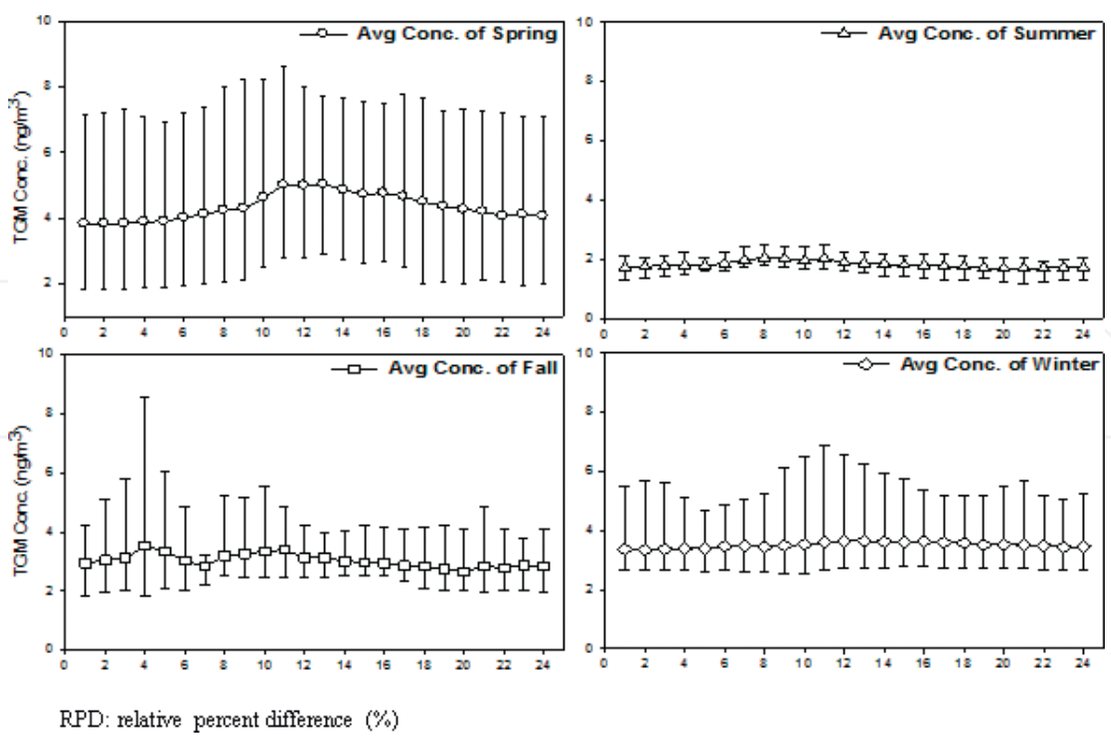

Figure 9. Frequency distribution of TGM concentration covering the four monitoring seasons.

for the morning time, the TGM concentration was less variable through the whole day. The average TGM concentrations in the daytime (6:00 am–6:00 pm) were typically higher than those at nighttime (6:00 pm–next 6:00 am). These findings are attributed to the effects from the variation of the height of atmospheric boundary layer. Additionally, it might be influenced by local anthropogenic activities, such as open burning, mobile sources of fishing boats, vehicles, etc.

The magnitude of hourly variation (differentia between the maximum and the minimum TGM concentrations) was lower in summer and winter with the relative percent differences (RPD) of 61.9 and 88.1%, respectively, and higher in spring and fall with the RPD of 130.7 and 107.8%, respectively. However, previous studies showed that the monitored TGM concentration varies at low altitudes in the typical rural areas [11, 21, 22]. This study revealed that the concentration of TGM monitored at the Penghu Islands was mainly influenced by both local biomass burning and long-range transportation.

Figure 10 illustrates the frequency distribution of TGM detected during four monitoring seasons. It showed that the TGM concentrations followed a lognormal distribution pattern in the range of 2.0–4.5 and 6.0–7.5 ng/m^3, accounting for approximately 80.0% of total frequency in spring. The values ranging from 1.5 to 2.5 ng/m^3 accounted for approximately 89.4% of total frequency in summer. Similarly, the values in the range of 2.0–4.5 and 3.5–5.5 ng/m^3 accounted for 93.3 and 61.7% of total frequency in fall and winter, respectively. However, the episodes with high TGM concentrations (>9.0 ng/m^3) were frequently observed in spring, fall, and winter. It is worth noting that the frequency distribution of TGM appeared to follow two different trends, as shown in **Figure 10**. The frequency distributions of TGM levels in summer and fall were unimodal distribution, while those in spring and winter followed a multi-modal distribution.

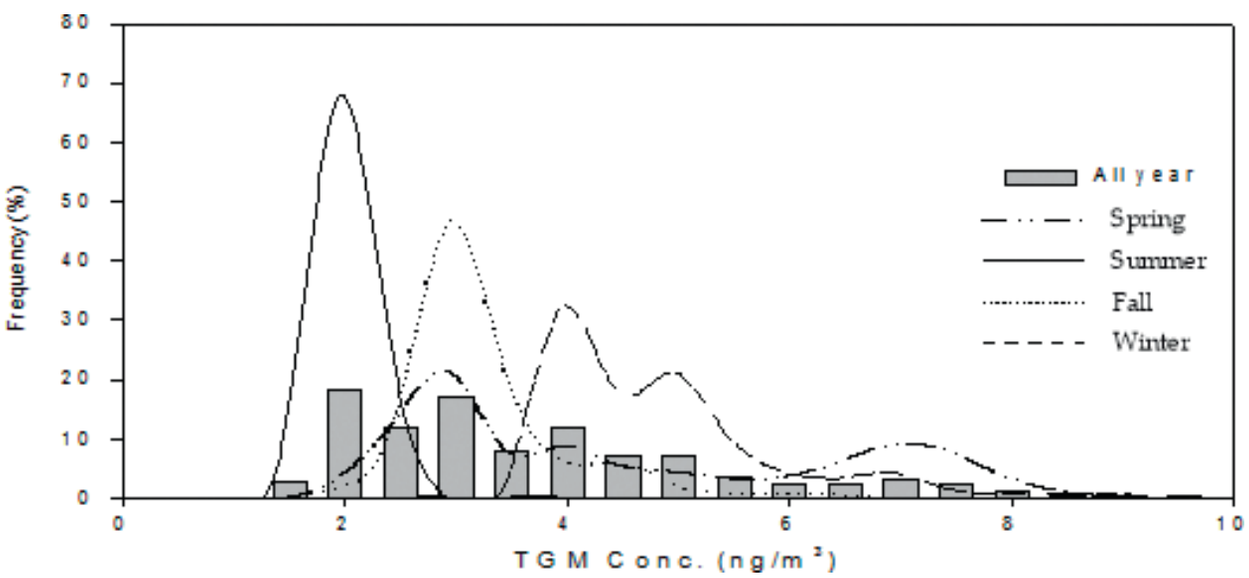

Figure 10. Pollution rose of TGM in four seasons at the Penghu Islands.

3.5. Transportation routes of TGM toward the Penghu Islands

Figure 11 illustrates the pollution rose of TGM for four monitoring seasons at the Penghu Islands. High TGM concentrations were observed mainly in the wind directions of 0–90° and followed by 270–360° in spring, and 60–120° in fall and winter. There were no significant mercury emission sources at the northwestern or southwestern Penghu Islands, suggesting that the high concentrations of TGM were transported remotely from China. An increasing number of studies have shown that biomass burning, industrial combustion, and ocean evaporation are three major emission sources of TGM in the regional scale [10, 23–25]. **Figure 12** illustrates the backward trajectories and the TGM concentration percentage of air masses toward the Penghu Islands in four seasons.

In spring, the TGM concentrations for air masses transported conveying from routes (1) and (2) ranged from 3.55–7.12 ng/m^3, accounting for approximately 89% of TGM data, which was possibly dominated by those transported from local stationary sources and open burning with air masses toward the Penghu Islands. Thus, the southern China were another possible sources contributing to the TGM levels at the Penghu Islands.

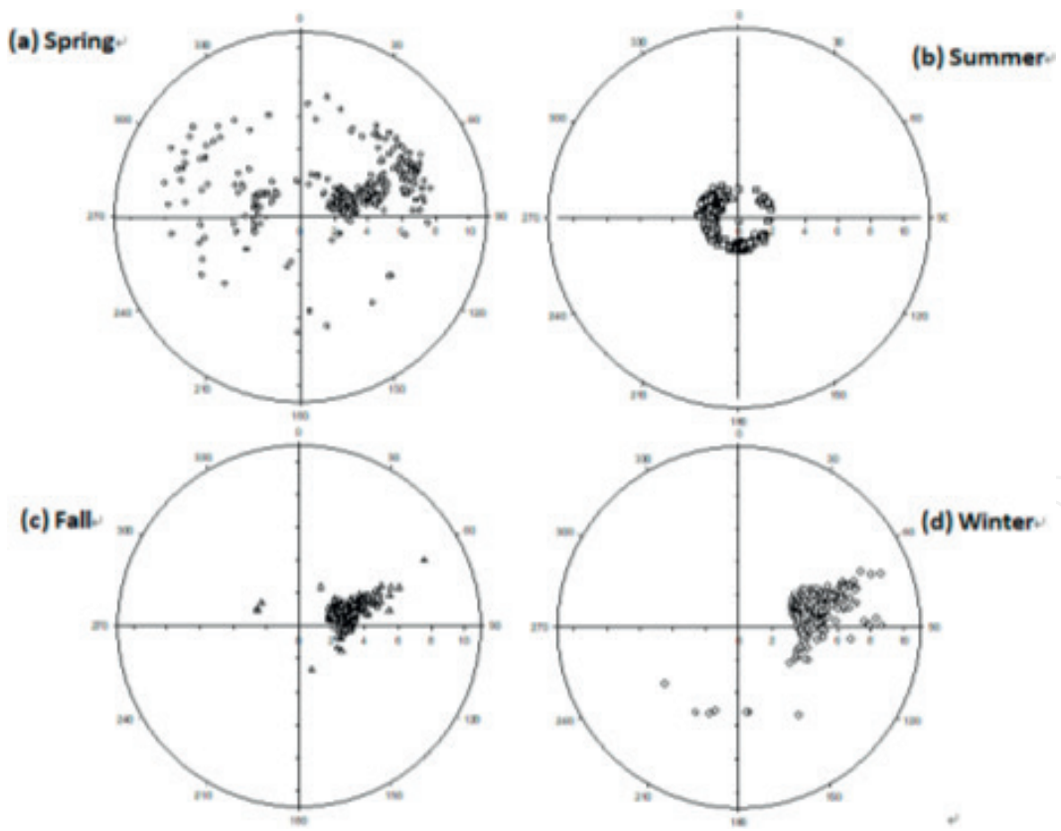

Figure 11. Backward trajectories of air masses and TGM concentration percentage for different pathways during the monitoring seasons at the Penghu Islands.

http://dx.doi.org/10.5772/intechopen.74051

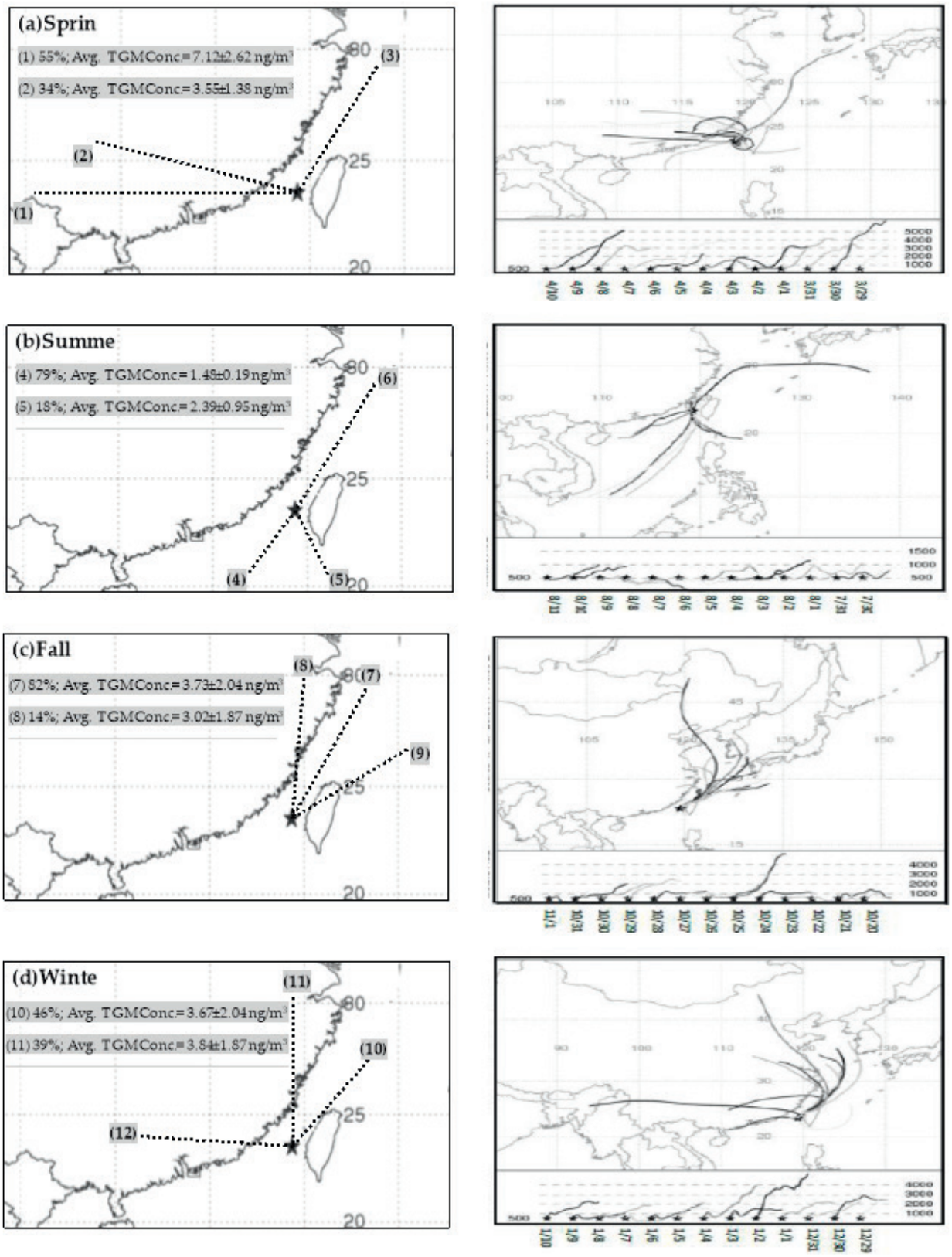

Figure 12. The percentage of the TGM concentration attributed from long-range transportation at the Penghu Islands.

In summer, the TGM concentrations for air masses conveying from routes (4) and (5) ranged from 1.48–2.39 ng/m^3, accounting for approximately 97% of TGM data, which were transported from the South and the East China Sea to the Penghu Islands, dramatically increasing the TGM concentrations at the Penghu Islands during the summer monitoring period. Consequently, the TGM concentrations in summer were relatively lower than other seasons, and the average concentration of TGM was close to the background TGM concentration of North Hemisphere (approximately 1.6 ng/m^3).

In fall, the TGM concentrations for the air masses conveying from routes (7) and (8) ranged from 3.02 to 3.73 ng/m^3, accounting for approximately 96% of TGM data, which seemed to be mainly transported from the northern China, Korea, and Japan with air masses toward the Penghu Islands, resulting in approximately 1.67 times higher TGM concentration in fall than those in summer.

In winter, the TGM concentrations for the air masses conveying from routes (11) and (12) ranged from 3.67 to 3.84 ng/m^3, accounting for approximately 85% of TGM data. The potential sources conveying the TGM toward the Penghu Islands in winter were from the southern Asia, northern China, and Mongolia, increasing the TGM concentrations up to 1.94 times of those in summer.

In this study, the minimum TGM value of 1.5 ng/m^3 in the summer monitoring period, can be treated as the background concentration of TGM at the Penghu Islands. Therefore, the TGM concentration attributed from long-range transportation can be obtained by Eq. (1), and illustrated in **Figure 13**:

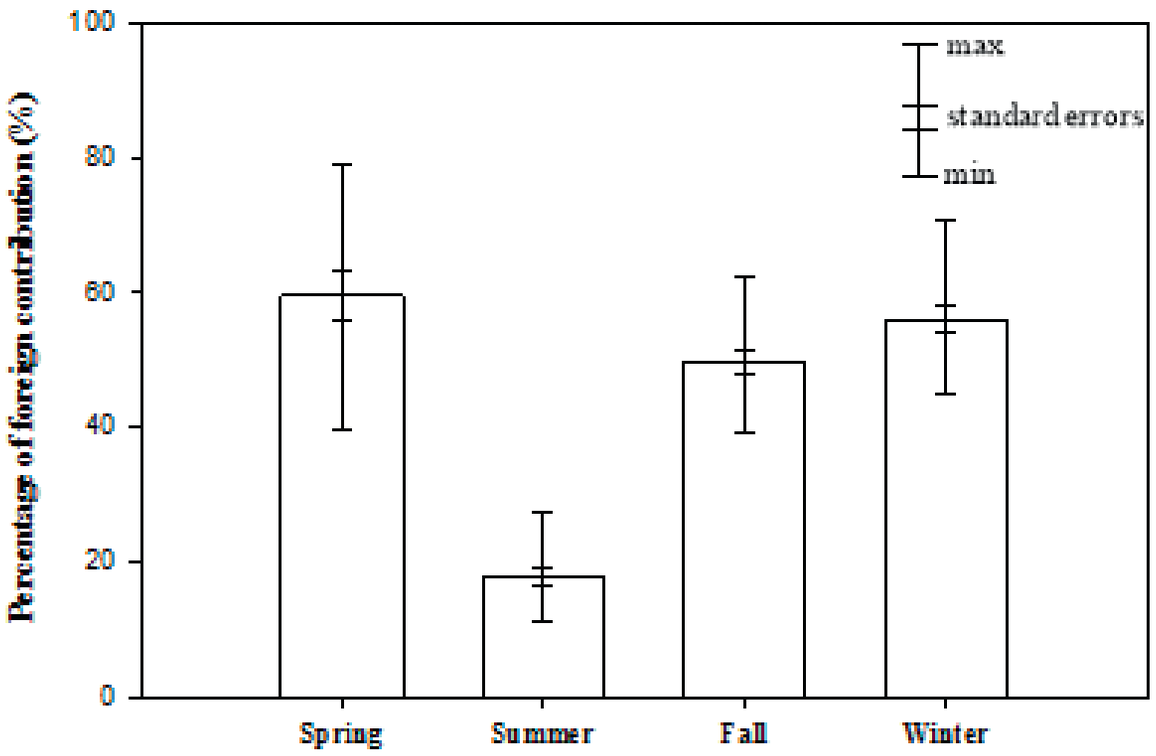

Figure 13. Fire maps air mass during four monitoring seasons in the East Asia in (a) spring, (b) summer, (c) fall, and (d) winter.

$$\text{Contribution percentage} = (\text{VMH} - \text{BC})/\text{VMH} \times 100\% \quad (1)$$

where contribution percentage is the TGM concentration attributed from cross-boundary transportation (%); VMH is the monitored TGM concentrations (ng/m^3); BC is the background concentration of Hg (i.e., 1.5 ng/m^3). The contribution percentage of TGM concentration attributed from cross-boundary transportation at the Penghu Islands were further compared. The percentages of cross-boundary transportation were ordered as: spring (59.6 ± 15.0%) > winter (55.9 ± 7.6%) > fall (49.7 ± 6.2%) > summer (16.8 ± 6.9%). In addition, the maximum percentage of 79.1% was observed in spring. It showed that the TGM concentrations in spring at the Penghu Islands were highly influential, which were mainly affected by the long-range transportation.

High humidity and rainfall frequency at the Penghu Islands could also explain relatively lower TGM concentrations measured in winter. Previous study reported that the occurrence of biomass burning such as forest fires from February to April in the Southeast Asia and the Indochina Peninsula emitting a large amount of mercury-containing pollutants to the atmosphere [26]. **Figure 14** illustrates the fire maps obtained from the FIRMS web fire maps and air mass transportation routes in four seasons. These fire maps explained why high TGM concentration occurred in spring at the Penghu Islands. During the monitoring periods, the hot spot of fires occurred densely in spring than other seasons could emit a large amount of TGM to the atmosphere, and then transported toward the Penghu Islands.

As illustrated in **Figure 15**, the TGM concentrations monitored at the Penghu Islands were compared to those observed at islands and seas in East Asia. The TGM concentrations in the ambient air were ordered as: An-Myun (4.61 ± 2.21 ng/m^3) > Jeju (3.85 ± 1.68 ng/m^3) > Penghu (3.17 ± 1.06 ng/m^3) > Yellow Sea (2.61 ± 0.50 ng/m^3) > South China Sea (2.32 ± 2.62 ng/m^3) > Okinawa Islands (2.04 ± 0.38 ng/m^3) [10, 22, 25–27]. The results showed that the TGM

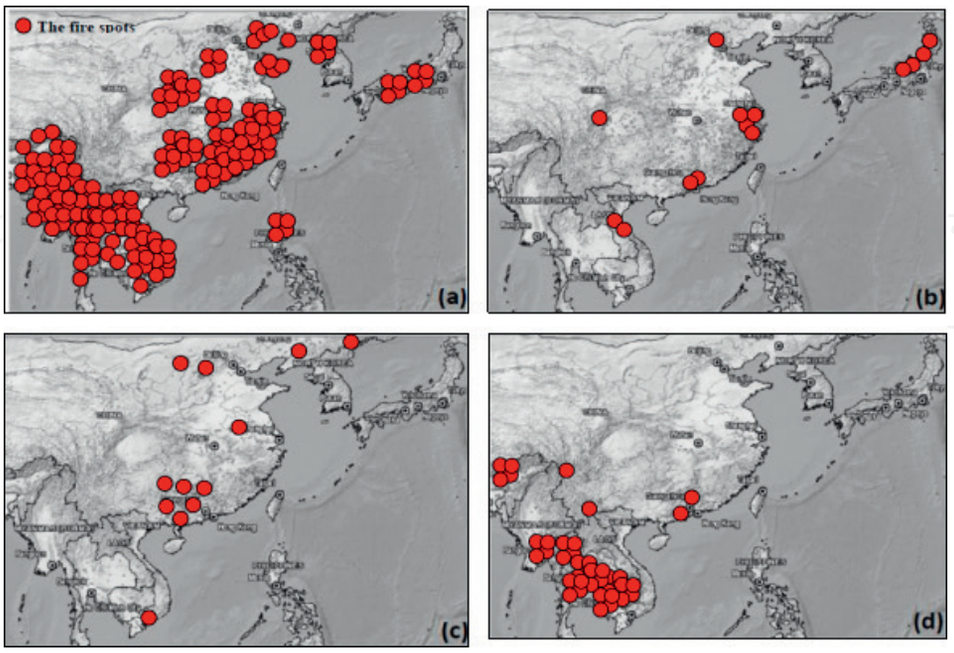

Figure 14. FThe concentration map of TGM at islands and seas in East Asia. (a) An-Myun Island (Nguyen et al., 2007); (b) Yellow Sea (Ci et al., 2011); (c) Jeju Island (Nguyen et al., 2010); (d) Okinawa Island (Chand et al., 2008); (e) Penghu Islands (This study); and (f) South China Sea (Fu et al., 2010).

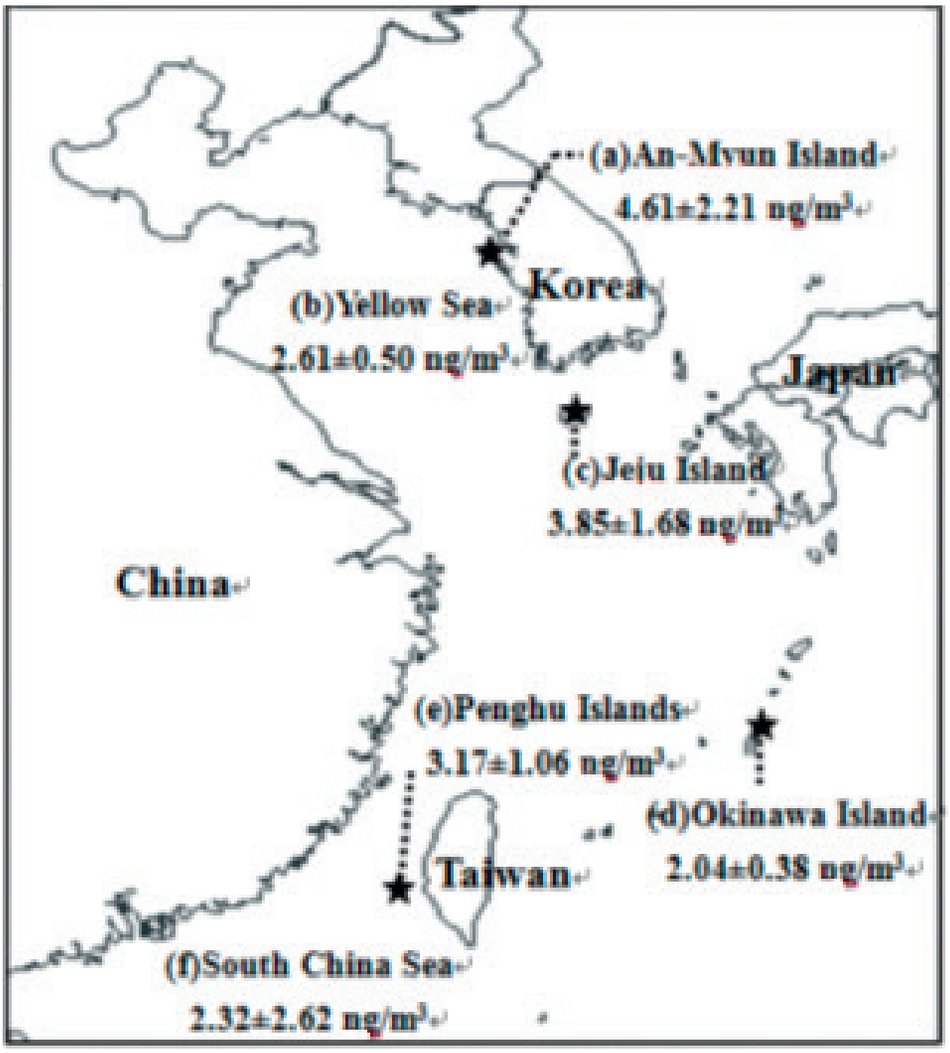

Figure 15. The concentration map of TGM at islands and seas in East Asia. (a) An-Myun Island; (b) Yellow Sea; (c) Jeju Island; (d) Okinawa Island; (e) Penghu Islands; and (f) South China Sea.

concentrations decreased continuously from the northern islands to the southern islands. The TGM concentrations observed at the offshore islands were generally lower than those close to the continent or main island (except Yellow Sea). It further explained why the high levels of TGM concentration at the offshore islands were much easily influenced by Hg emission sources from the anthropogenic sources in the continent or main island.

In summary, in addition to the local sources and open burning, the concentration of TGM at the Penghu Islands was mainly influenced by the long-range transportation of air masses, as the prevailing wind direction and air mass transportation routes potentially playing the critical roles on the variation of TGM concentration in the atmosphere.

4. Conclusions

This chapter investigated the atmospheric mercury by using the modified sampling and analytical methods from two cases of small-scale regions to large-scale regions, respectively,

which further investigated the tempospatial variation of atmospheric mercury, gas-particulate partition, transportation routes of mercury, and comparison of mercury concentration in urban areas and stationary sources. According to the results of this field study, several major conclusions are summarized as follows.

The tempospatial variation and the partition of TGM and Hg_p in Kaohsiung City were 6.66 ± 1.42 ng/m^3 and 0.29 ± 0.21 ng/m^3, respectively. The TGM concentration was approximately 4.1 times higher than the background concentration of 1.6 ng/m^3 in North Hemisphere. Two high mercury concentration regions in Kaohsiung City concurred with the petrochemical complex in Northern Kaohsiung, and the steel manufacturing complex in Southern Kaohsiung.

The TGM and Hg_p concentrations in Kaohsiung City were generally higher than those of other Taiwanese cities during the wet and dry seasons. The concentrations of TGM measured in the cities of Taiwan were generally higher than Tokyo and Seoul, however, lower than other cities in China. The burning of coal for space heating in wintertime makes China the main mercury emission source in the world. Moreover, Japan, Korea, and Taiwan are under the leeward of China, which are also in the major atmospheric mercury transportation routes. When the northeastern monsoon prevails, it resulted in the increase of TGM and Hg_p concentrations in the cities of East Asia.

TGM concentration monitored at the Penghu Islands was 3.17 ± 1.06 ng/m^3 with the range of 1.17–8.63 ng/m^3, and were ordered as: spring > winter > fall > summer. Summer is the only season close to the background TGM concentration of Northern Hemisphere at the Penghu Islands. While the hourly variation, TGM concentration typically increased in the morning (8:00 am–1:00 pm), reached its peak concentration, and then decreased in the late afternoon (after 2:00 pm).

Air masses transported from the southern and northern China, the southern Asia, Korea, Japan, and Mongolia might affect the Hg levels at the Penghu Islands during the monitoring seasons. The concentrations of TGM might be influenced by the mercury-polluted air masses to be transported remotely from areas or local stationary combustion and mobile sources. While air masses transported toward the Penghu Islands was dominated by that transported from South China Sea in summer, the TGM concentration levels at the Penghu Islands appeared to be lower than other seasons.

High TGM concentration observed at the Penghu Islands in spring might be attributed to the following three reasons: (a) local emissions from field open burning, local stationary combustion, and mobile sources; (b) long-range transportation from biomass burning in Southeast Asia or neighboring Chinese coastal cities, and (c) long-range transportation through Asian dusts from North China.

Acknowledgements

The authors gratefully acknowledge the financial support and kind assistance from National Sun Yat-Sen University of Air Pollution Control Laboratory (APCL). The authors would like to express their sincere appreciation for its financial support to accomplish this study.

Author details

Yi-Hsiu Jen and Chung-Shin Yuan*

*Address all correspondence to: ycsngi@mail.nsysu.edu.tw

Institute of Environmental Engineering, National Sun Yat-Sen University, Kaohsiung City, Taiwan, ROC

References

[1] UNEP. Global Mercury Assessment, December. 2002. http://www.chem.unep.ch/mercury/report/gma-report-toc.htm

[2] UNEP. Part a: Global Emissions of Mercury to the Atmosphere, UNEP/AMAP 2012 Technical Report, July. 2012

[3] Nater EA, Grigal DF. Regional trends in mercury distribution across the Great Lakes states, north central USA. Nature. 1992;**358**:139-141

[4] Mason RP, Fitzgerald WF, Morel MM. The biogeochemical cycling of elemental mercury: Anthropogenic influences. Geochimica et Cosmochimica Acta. 1994;**58**:3191-3198

[5] Mason RP, Sheu GR. Role of the ocean in the global mercury cycle. Global Biogeochemical Cycles. 2002;**16**(4):1093-1107

[6] Schroeder WH, Munthe J. Atmospheric mercury—An overview. Atmospheric Environment. 1998;**32**:809-822

[7] Lin CJ, Pehkonen SO. The chemistry of atmospheric mercury: A review. Atmospheric Environment. 1999;**33**:2067-2079

[8] Boening DW. Ecological effects, transport, and fate of mercury: A general review. Chemos. 2000;**40**:1335-1351

[9] Clarkson TW, Magos L. The toxicity of mercury and its compounds. Critical Reviews in Toxicology. 2006;**36**:609-662

[10] Fu XW, Feng XB, Dong ZQ, Yin RS, Wang JX, Tang ZR, Zhang H. Atmospheric gaseous elemental mercury (GEM) concentrations and mercury depositions at a high-altitude mountain peak in south China. Atmospheric Chemistry and Physics Discussions. 2010;**9**:23465-23504

[11] Sheu GR, Lin NH, Wang JL, Lee CT, Ou CF, Yang CFO, Wang SH. Temporal distribution and potential sources of atmospheric mercury measured at a high-elevation background station in Taiwan. Atmospheric Environment. 2010;**44**:2393-2400

[12] Jen YH, Yuan CS, Lin YC, Lee CG, Hung CH, Tsai CM, Tsai HH, Ie IR. Partition and tempospatial variation of gaseous and particulate mercury at a unique mercury-contaminated remediation site. Journal of the Air & Waste Management Association. 2011;**61**:1115-1123

[13] Jen YH, Yuan CS, Hung CH, Ie IR, Tsai CM. Tempospatial variation and partition of atmospheric mercury during wet and dry seasons at sensitivity sites within a heavily polluted industrial city. Aerosol and Air Quality Research. 2013;**13**:13-23

[14] Poissant L, Pilote M, Beauvais C, Constant P, Zhang HH. A year of continuous measurements of three atmospheric mercury species (GEM, RGM, and Hg_p) in Southern Quebec, Canada. Atmospheric Environment. 2005;**39**:1275-1287

[15] Feng XB, Tang SL, Shang LH, Yan HY, Sommar J, Lindqvist O. Total gaseous mercury in the atmosphere of Guiyang, PR China. Science of the Total Environment. 2003;**304**:61-72

[16] Fu X, Feng X, Zhu W, Zheng W, Wang S. Total particulate and reactive gaseous mercury in ambient air in the eastern slope of Mt. Gongga area. Applied Geochemistry. 2008;**23**(3):408-418

[17] Sheu GR, Mason RP. An examination of methods for the measurements of reactive gaseous mercury in the atmosphere. Environmental Science & Technology. 2001;**35**(6):1209-1216

[18] Sheu GR, Lin NH, Wang JL, Lee CT. Monitoring of atmospheric mercury concentration at surface sites in Taiwan. Atmospheric Chemistry and Physics. 2009;**30**:1-10

[19] Yuan CS, Lin HY, Wu CH, Liu MH. Preparing of sulfurized powdered activated carbon from waste tires using an innovative compositive impregnation process. Journal of the Air & Waste Management Association. 2004;**54**:862-870

[20] Stamenkovic J, Lyman S, Gustin MS. Seasonal and diel variation of atmospheric mercury concentrations in the Reno (Nevada, USA) Airshed. Atmospheric Environment. 2007;**41**:6662-6672

[21] Mao H, Talbot R. Speciated mercury at marine, coastal, and inland sites in New England—Part 1: Temporal variability. Atmospheric Chemistry and Physics Discussions. 2011;**11**:32301-32336

[22] Nguyen HT, Kim MY, Kim KH. The influence of long-range transport on atmospheric mercury on Jeju Island, Korea. Science of the Total Environment. 2010;**408**(6):1295-1307

[23] Blanchard P, Froude FA, Martin JB, Clark HD, Woods JT. Four years of continuous total gaseous mercury (TGM) measurements at sites in Ontario, Canada. Atmospheric Environment. 2002;**36**:3735-3743

[24] Chand D, Jaffe D, Prestbo E, Swartzendruber PC, Hafner W, Penzias PW, Kato S, Takami A, Hatakeyama S, Kajii Y. Reactive and particulate mercury in the Asian marine boundary layer. Atmospheric Environment. 2008;**42**:7988-7996

[25] Ci ZJ, Zang XS, Wang ZW, Niu ZC, Diao XY, Wang SW. Distribution and air-sea exchange of mercury (Hg) in the Yellow Sea. Atmospheric Chemistry and Physics Discussion. 2011;**11**:2881-2892

[26] Sigler JM, Lee X, Munger W. Emission and long-range transport of gaseous mercury from a large-scale Canadian boreal forest fire. Environmental Science & Technology. 2003;**37**:4343-4347

[27] Nguyen H, Kim KH, Kim MY, Hong S, Youn YH, Shon ZH, Lee J. Monitoring of atmospheric mercury at a global atmospheric watch (GAW) site on An-Myun Island, Korea. Water, Air, & Soil Pollution. 2007;**185**:149-164

IntechOpen